Evidence for phase separation of ethanol-water mixtures at the hydrogen terminated nanocrystalline diamond surface

Stoffel D. Janssens, Sien Drijkoningen, Marc Saitner, Hans-Gerd Boyen, Patrick Wagner, Karin Larsson, and Ken Haenen

Citation: The Journal of Chemical Physics **137**, 044702 (2012); doi: 10.1063/1.4738192
View online: http://dx.doi.org/10.1063/1.4738192
View Table of Contents: http://scitation.aip.org/content/aip/journal/jcp/137/4?ver=pdfcov
Published by the AIP Publishing

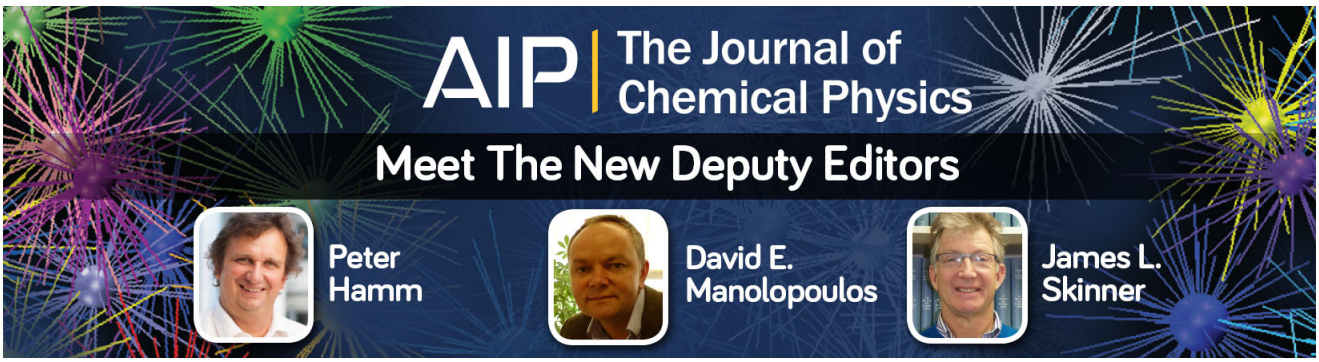

Evidence for phase separation of ethanol-water mixtures at the hydrogen terminated nanocrystalline diamond surface

Stoffel D. Janssens,[1,2,a)] Sien Drijkoningen,[1] Marc Saitner,[1] Hans-Gerd Boyen,[1] Patrick Wagner,[1,2] Karin Larsson,[3] and Ken Haenen[1,2,b)]
[1]*Institute for Materials Research (IMO), Hasselt University, Wetenschapspark 1, 3590 Diepenbeek, Belgium*
[2]*IMOMEC, IMEC vzw, Wetenschapspark 1, 3590 Diepenbeek, Belgium*
[3]*Department of Chemistry - Ångström Laboratory, Uppsala University, Box 538, Uppsala 751 21, Sweden*

(Received 27 April 2012; accepted 6 July 2012; published online 23 July 2012)

Interactions between ethanol-water mixtures and a hydrophobic hydrogen terminated nanocrystalline diamond surface, are investigated by sessile drop contact angle measurements. The surface free energy of the hydrophobic surface, obtained with pure liquids, differs strongly from values obtained by ethanol-water mixtures. Here, a model which explains this difference is presented. The model suggests that, due to a higher affinity of ethanol for the hydrophobic surface, when compared to water, a phase separation occurs when a mixture of both liquids is in contact with the H-terminated diamond surface. These results are supported by a computational study giving insight in the affinity and related interaction at the liquid-solid interface. © *2012 American Institute of Physics*. [http://dx.doi.org/10.1063/1.4738192]

I. INTRODUCTION

In contrast to the hydrogen terminated silicon surface,[1] the hydrogen terminated diamond surface is not easily undergoing chemical changes,[2] and therefore plays an important role in a wide variety of studies. Ranging from surface-conductive field-effect transistors,[3,4] thermionic emission devices,[5–7] to the starting point for many functionalisation experiments leading to novel biosensor concepts.[8–10] In many of these situations, the diamond surface is in contact with a fluid. This can be pure water, but also buffer solutions or (aggressive) mixtures for electrochemical experiments are used. Dankerl *et al.*[11] recently showed that the hydrophobic nature of the surface can have a profound effect on device working based on the behaviour of water on the surface.

The behaviour of alcohol-water mixtures is non-trivial to examine due to complex interactions between alcohol-alcohol, alcohol-water and water-water molecules. It is observed that the entropy of mixtures is far less than for ideal mixtures.[12] This is experimentally explained by incomplete mixing, i.e., hydrogen-bond chain and ring structure formations.[13,14] Computational studies support the existence of these structures and increasingly shed more light on the microstructural behaviour.[15,16] On hydrophilic SiO_2 and mica surfaces, Kanda *et al.*[17] already studied alcohol-water mixtures, proposing that a monolayer of alcohol molecules can be formed on the hydrophilic surface. In their model the hydroxyl groups of the alcohol molecules interact with the hydrophilic surface with the alkyl groups pointing in the direction of the high alcohol containing solution.

Here, the interactions between ethanol-water mixtures and a hydrophobic surface, i.e., hydrogen terminated nanocrystalline diamond films (NCD:H), are investigated by sessile drop contact angle measurements (CA). With the "Owens, Wendt, Rable, and Kaelble" method (OWRK) the surface free energy value (γ), and its polar/disperse parts (γ^P, γ^D), are calculated after performing CA measurements with pure liquids and with ethanol-water mixtures. Mixtures are known to lead to erroneous γ values,[18] which will be confirmed in this work. It will be shown that γ derived with mixtures is about half the value of γ derived with pure liquids. Pure liquid CA experiments also show that γ^P is zero for hydrophobic surfaces. A model to explain the differences in the surface free energies obtained by pure liquids and alcohol-water mixtures is proposed and supported by theoretical calculations.

II. EXPERIMENTAL

A. Nanocrystalline diamond

Five intrinsic NCD samples of 1 cm by 1 cm are grown on pretreated silicon substrates with a microwave plasma enhanced chemical vapour deposition process.[19] Growth was performed in a commercial ASTeX 6500 series reactor during 23 min with a 2% C/H-ratio, a pressure of 30 Torr and a temperature of 815 °C, as monitored with a Williamson Pro92 dual wavelength pyrometer. When a thickness of 150 nm was reached, growth was stopped. Post growth hydrogenation takes place right before each contact angle measurement to avoid surface contamination and oxidation of the surface under ambient conditions. A process also described by Kim *et al.*[20] is used to ensure full hydrogen surface termination. An x-ray photoelectron spectroscopy (XPS) spectrum, was taken in order to investigate surface impurities. The spectrum was measured using a commercial photoemission system (Physical Electronics PHI 5600 LS). The spotsize of the beam was 1.1 mm and the overall energy-resolution

a)Electronic mail: stoffel.janssens@uhasselt.be.
b)Electronic mail: ken.haenen@uhasselt.be.

smaller than 0.4 eV (FWHM). Eventually, CA measurements were performed with a DataPhysics OCA 15 plus device.

B. The "OWRK" method

In the "OWRK" method, the surface free energy consists of polar contributions (γ^P) and disperse contributions (γ^D)

$$\gamma = \gamma^P + \gamma^D \tag{1}$$

and with the following relations, it is possible to construct a line equation ($Y = AX + B$) with A the slope, B the intercept and X the independent variable of function Y

$$Y = \frac{\gamma_{LV}(\cos\theta + 1)}{2\sqrt{\gamma^D_{LV}}}, \tag{2}$$

$$A = \sqrt{\gamma^P_{SV}}, \tag{3}$$

$$X = \sqrt{\frac{\gamma^P_{LV}}{\gamma^D_{LV}}}, \tag{4}$$

$$B = \sqrt{\gamma^D_{SV}}, \tag{5}$$

which is the so-called "OWRK" plot. LV stands for liquid/vapor, SV stands for solid/vapor, and θ stands for the contact angle. Figure 1(a) graphically shows θ of a water droplet on a NCD:H surface and Fig. 1(b) is an illustration of the use of the "OWRK" method in determining γ. For a solid, the polar part of γ can be calculated from the slope and the disperse part of γ can be calculated from the intercept of the "OWRK" plot. At least two points (X_1, Y_1) and (X_2, Y_2) need to be plotted to do this and therefore, the contact angles (θ_1, θ_2) between the solid and two different liquids have to be measured. It is clear that this method requires the polar and the disperse parts of γ of the liquids to be known.

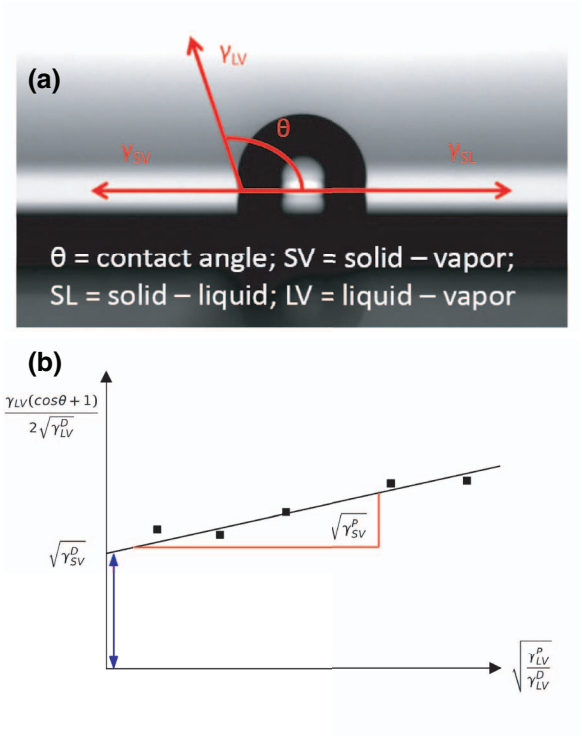

FIG. 1. In panel (a), a sessile water droplet on a NCD:H surface with the surface energies and contact angle presented. The lengths of the vectors do not correspond to the real values of surface energies. In panel (b), an illustration of the use of the "OWRK" method in determining the surface energy.

In the first type of experiment γ of NCD:H is derived using pure liquids with known polar and disperse γ parts. Such experiments are done with water, ethylene glycol, and diiodomethane. In the second series of experiments the surface free energy of NCD:H is derived using ethanol-water mixtures (0, 10, 20, 30, 40, 50, 60, and 70 vol. % ethanol). The surface free energy of the mixtures are reported by Vazquez *et al.*,[21] although this does not include the polar and disperse parts. To derive these, additional measurements, comparable with the experiments of Chen and Hong,[22] were performed on a set of polymers (PA, PC, PE, PMMA, PS, PTFE, PVC).

C. Computational study

In order to estimate the interactions of NCD:H and ethanol-water mixtures, the affinity of water and ethanol for the (111) and (100) NCD:H surfaces is calculated by means of first principle functional theory (DFT) calculations. The adhesion energies for water vs. ethanol in contact with an H-terminated diamond surface, were calculated using all-electron DFT, as implemented in the program package DMol^3 (Materials Studio) from Accelrys, incorporation. All calculations were performed with the generalized gradient approximation using the PW91 functional and the double numeric basis set with polarization functions.[23] The Brillouin zone was sampled with a (221) Monkhorst-Pack grid.[24] Van der Waals interaction between the adlayer (water or ethanol) and the diamond surface were accounted for by using the OBS dispersion correction.[25] The water adlayers were initially constructed using four H_2O layers from the cubic phase of ice, followed by complete structural relaxation of the adlayers.

It is practical impossible to perform these high-level calculations on model sizes larger than approximately 3 nm in diameter. Moreover, the surface of NCD is comprised of different facets of diamond, and the most common ones are (111) and (100). Hence, the H-terminated diamond (111) and (100) surfaces have in the present work been used as representative nano-sized surface parts of NCD:H, and were therefore modeled as super cells under periodic boundary conditions. The size of the super cell varied depending on the adlayer type. The smallest repeatable unit consists of 6 C layers, with H-terminated upper and lower C layers. It has earlier been shown adequate to use this number of layers when studying weaker surface reactions like the present ones.[26] Both x and y axis are of identical length, and the vacuum layer was set to 17 Å. The positions of the atoms within the bottom C layer, plus the dangling bond-passivating H atoms, were fixed during the calculations to simulate the structure of bulk diamond. The rest of the atoms were allowed to fully relax using the Broyden-Fletcher-Goldfarb-Shanno algorithm.[27]

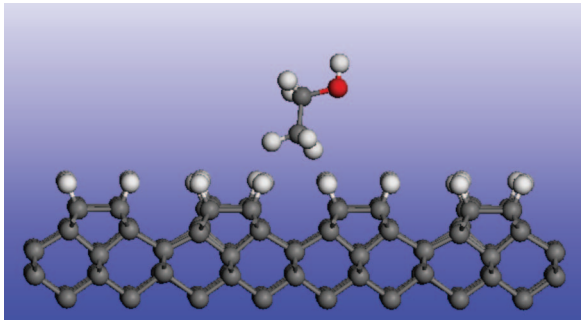

FIG. 2. Demonstration of the periodic model used for simulating the adhesion of either ethanol or water onto an H-terminated diamond (100)-2 × 1 facet. The lower H-termination is removed for clarity.

Three different starting configurations were used for the water molecule on the NCD:H surface; with (I) O pointing in the direction towards the surface, (II) both H atoms towards the surface, or (III) only one of the H atoms towards the surface. The energetically most preferred orientation was structure type II), reflecting the strongest hydrophobic-hydrophobic interaction between the surface and the water molecule. For the situation with ethanol, two different initial geometries were tested; with (I) the hydrophobic methyl group towards the surface (Fig. 2), or (II) the hydrophilic OH group towards the surface. The energetically most preferred orientation was also here type II), but with the final orientation that promotes a hydrophobic-hydrophobic interaction.

III. RESULTS AND DISCUSSION

Figure 3(a) shows a scanning electron microscopy (SEM) image of an as-grow NCD:H film used in this work. All five films are investigated by SEM and none of them contained pinholes. The XPS spectrum in Fig. 3(b) shows besides the carbon peaks, very small signals of fluorine and oxygen (≈1%) demonstrating the very low level of contaminations.

Figure 4(a) is the "OWRK" plot of the contact angle measurements on the 5 NCD:H samples. On each sample, 3 droplets of pure liquids (mentioned above) are deposited, resulting in 15 measurements. After averaging, 3 data points with very low errors (<5%) remain. From the least squares fit, γ (34 ± 5 mN/m), γ^P (0.1 ± 0.3 mN/m), and γ^D (34 ± 5 mN/m) are calculated. The value of the total surface free energy is in tune with the value obtained by Azevedo *et al.*[28] for high quality NCD:H.

To determine γ of the ethanol-water mixtures, γ of the polymers are calculated after CA measurements with pure liquids on the polymers. These values are listed in Table I. Then, γ of the ethanol-water mixtures are determined after performing CA measurements with the mixtures on the polymers. These values are listed in Table II. Figure 4(b) is the "OWRK" plot for the CA measurements of the ethanol-water mixtures on NCD:H. Mixtures with higher ethanol concentrations lead to unmeasurable low contact angles on the polymers and sometimes also droplets with non-circular shapes were formed. These data points were not included for further study. From the least squares linear fit performed on Fig. 4(b), γ (16 ± 4 mN/m), γ^P (7 ± 2 mN/m), and γ^D (9 ± 4 mN/m) are calculated. The surface free energy is about 50% lower than with the pure liquids and the polar part is highly significant. The obtained values of the surface free energy are summarised on Fig. 5. This observed polar part exists from polar interactions of the mixture with the surface. Compared with the zero value for γ^P obtained by pure liquids, more polar interactions should be present on the NCD:H surface when measuring with the mixtures. Kanda *et al.*,[17] already suggested the formation of a monolayer of alcohol molecules on a hydrophilic surface when it is covered with

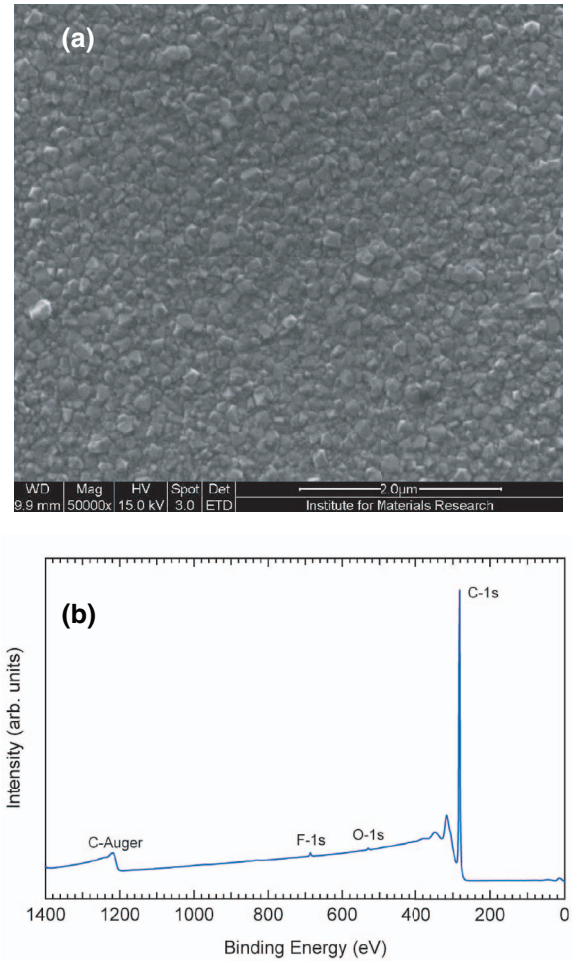

FIG. 3. In panel (a), a scanning electron microscopy image of a pinhole free NCD:H film. In panel (b), an XPS spectrum of one NCD:H sample with a small oxygen and fluorine signal next to a clear carbon peak.

TABLE I. Surface energies of polymers, calculated after performing CA measurements with ethylene glycol, diiodomethane, and water.

Polymer	γ^D (mN/m)	γ^P (mN/m)
PA	34.0	8.0
PC	40.7	0.1
PE	27.0	0.2
PMMA	32.0	0.6
PS	31.0	2.0
PTFE	0.0	7.9
PVC	36.9	0.1

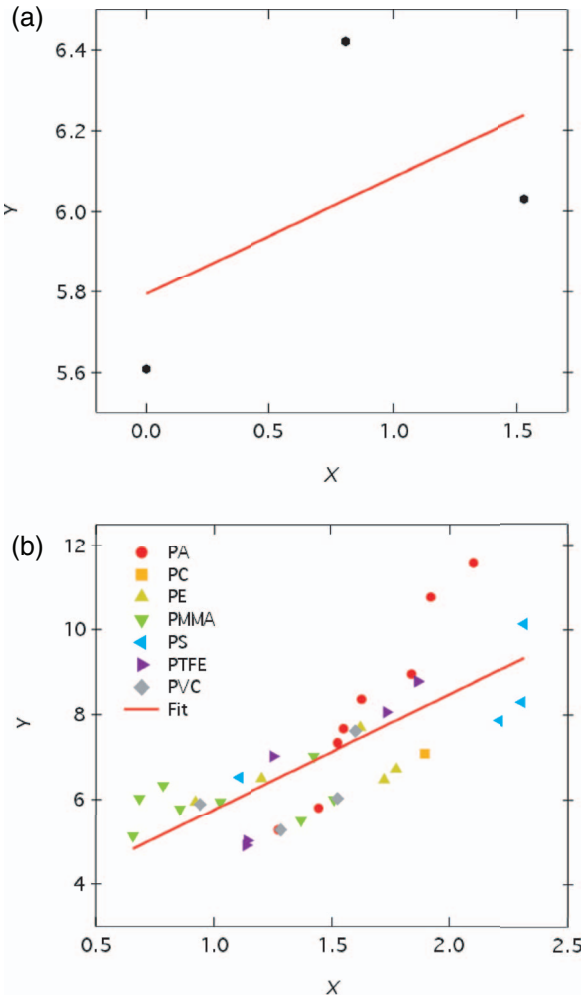

FIG. 4. In panel (a), the OWRK plot of the contact angle measurements on NCD:H with pure liquids and in panel (b), the OWRK plot of the contact angle measurements on NCD:H with ethanol-water mixtures. On both graphs, *Y* refers to Eq. (2) and *X* refers to Eq. (4). Each data point represents an averaged value derived from 5 NCD:H samples. Since the errors on these points are very small, they are not presented.

TABLE II. Contact angles of a series of ethanol-water mixtures on different polymer surfaces. The disperse and polar surface energies of the mixtures are calculated using the values in Table I. Values for *X* and *Y* are calculated using Eqs. (2) and (4) and are then plotted in Fig. 4(b).

	Ethanol-water (Vol. %)	CA (°)	γ^D (mN/m)	γ^P (mN/m)	*X*	*Y* (mN/m)$^{1/2}$
PA	0	71	24	49	1.4	5.8
	10	52	20	32	1.3	5.2
	20	42	12	29	1.5	7.3
	30	31	10	25	1.6	7.7
	40	24	9	24	1.6	8.4
	50	25	7	24	1.8	9.0
	60	19	6	23	1.9	10.8
	70	17	5	22	2.1	11.6
PC	0	103	16	57	1.9	7.1
PE	0	108	18	55	1.8	6.7
	10	100	13	39	1.7	6.5
	20	92	11	30	1.6	7.7
	30	77	14	21	1.2	6.5
	40	64	18	15	0.9	5.9
PMMA	0	97	22	50	1.5	6.0
	10	84	18	34	1.4	5.5
	20	78	13	27	1.4	7.0
	30	59	17	18	1.0	5.9
	40	47	19	14	0.9	5.8
	50	30	21	9	0.7	5.1
	60	24	20	9	0.7	6.0
	70	25	17	10	0.8	6.3
PS	0	100	12	61	2.3	8.3
	10	90	9	43	2.2	7.9
	20	84	6	34	2.3	10.1
	40	48	15	18	1.1	6.5
PTFE	0	118	32	41	1.1	5.0
	10	112	23	29	1.1	4.9
	20	102	10	31	1.7	8.0
	30	98	8	28	1.9	8.8
	40	101	13	20	1.3	7.0
PVC	0	99	22	51	1.5	6.0
	10	84	20	32	1.3	5.3
	20	85	11	29	1.6	7.6
	50	48	16	14	0.9	5.9

alcohol-water mixtures. It is stated that the polar parts of the alcohol molecules interact with the surface and the hydrophilic groups point towards the solution. The experimental data in this work strongly suggests a similar model for alcohol-water mixtures on a NCD:H surface. Since alcohol molecules have a polar (hydrophylic) and a disperse (hydrophobic) region, it is highly possible that the disperse region makes the ethanol more attracted to the NCD:H which can lead to a phase separation on the NCD:H surface. This phase separation leads to a NCD:H surface with a higher ethanol concentration on top of it and explains the polar interactions which are measured.

In the computational study, the affinity of ethanol and water for NCD:H is determined by calculating the adhesion energy between water (or ethanol) and the H-terminated diamond (111) and (100)-2×1 surfaces, respectively. (Figure 2 demonstrates the adhesion of one ethanol molecule onto an H-terminated diamond (100)-2×1 facet.) Two different models were tested; (I) one water (or ethanol) molecule, or (II) a very thin water adlayer (or a monolayer of ethanol). The former model tested the interaction between the individual molecules (water or ethanol) and the hydrophobic diamond surface, and the latter included also the effects of neighbouring molecules via H-bonding and/or van der Waals interactions. However, very similar results were obtained irrespective of number of molecules in the adlayer (see Table III). Hence, it was considered not necessary to use even thicker adlayer systems in the calculations.

The main conclusion from the calculations is that ethanol will bind much stronger to the hydrophobic NCD:H than water does; with a factor of approximately two. This relative preference is almost identical for both the (111) and (100) facets on the NCD surface. However, the reactivity towards adhesion (for both ethanol and water) is somewhat more pronounced for the H-terminated (111) surface planes. We have earlier shown theoretically that the (111) surface is

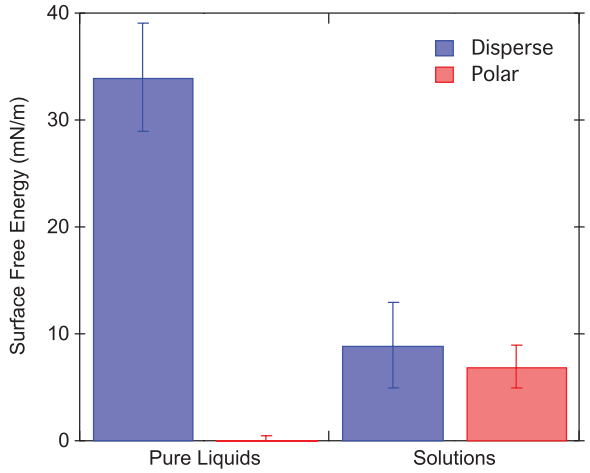

FIG. 5. Surface energy values for NCD:H measured with pure liquids and solutions. The polar contribution of the surface energy is negligible for the measurement with pure liquids. The high polar surface energy contribution for the measurement with solutions.

more reactive towards surface termination with hydrogen or oxygen species.[29]

In addition, to test if the hydrophobic alkyl groups of the ethanol molecules have a higher affinity for the hydrophobic NCD:H surface, two different models were used. The calculations were either initiated by positioning the ethanol molecule with the hydrophobic part towards the hydrophobic H-terminated surface (Fig. 2), or with the hydrophilic OH group towards the surface (Fig. 6(a)), and allowing the atoms to completely relax (i.e., perform geometry optimization). As a result, the initial model with the alkyl group towards the surface, did not change much as a result of the relaxation. For the other model with the OH group towards the surface (and with the partially negative O towards the slightly positive H species on the surface), the ethanol molecules switched position to a final one with the partially positive H atoms (in the ethanol) directed towards the surface H species. The corresponding calculated adhesion energies showed a largely improved stability in favour of the hydrophobic interaction (Fig. 6(b)). These theoretical results do strongly support the experimental observations made in the present study.

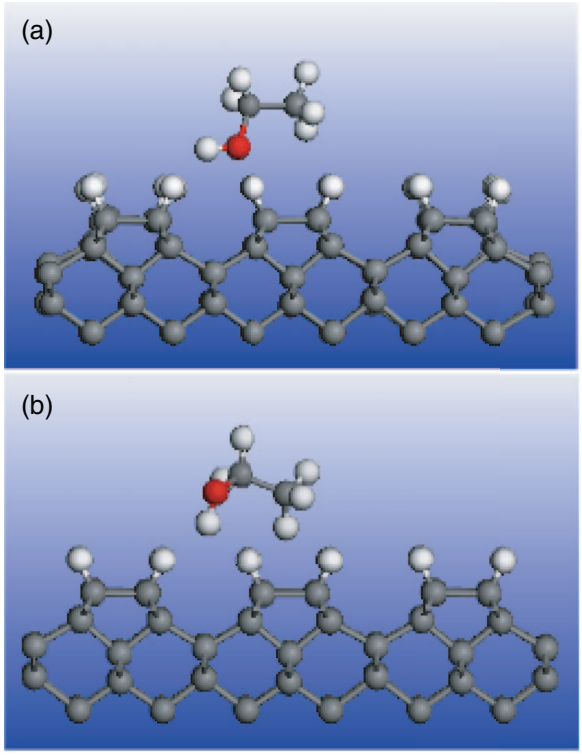

FIG. 6. Periodic model showing an (a) initial, and (b) optimized, model used for simulating the adhesion of ethanol onto an H-terminated diamond (100)-2×1 facet.

TABLE III. Calculated adhesion energy per ethanol or water molecule being attached to the NCD:H surface. The values within parentheses are for one monolayer of ethanol, or for a very thin water adlayer. The others are the result of only one ethanol (or water) molecule attached to the surface.

Surface orientation	Ethanol (kJ/mol)	Water (kJ/mol)
(100)-2×1	129 (138)	60 (50)
(111)	158	89

IV. CONCLUSIONS

The surface free energy of NCD:H, obtained by performing contact angle measurements with pure liquids and with ethanol-water mixtures, is evaluated by means of the OWRK method (34 ± 5 mN/m). The measurements with pure liquids only show disperse interactions with the NCD:H surface. In contrary, the measurements with mixtures result in a different surface free energy value (16 ± 4 mN/m). Also polar interactions (7 ± 2 mN/m) with the NCD:H surface are now clearly present. A model to explain these results is suggested and states that a phase separation of the ethanol-water mixture at the NCD:H surface is responsible for the observation of polar interactions. This is supported by DFT calculations by which the adhesion of ethanol and water onto different oriented H-terminated diamond surfaces is compared. For all surface orientations, it is calculated that the adhesion of ethanol is much higher than the adhesion of water which supports the proposed model.

ACKNOWLEDGMENTS

This work was financially supported by the EU FP7 Marie Curie ITN "MATCON" (PITN-GA-2009-238201), the Collaborative Project "MOLESOL" (No. 256617), and the Research Foundation-Flanders (FWO) (G.0555.10N).

[1]B. Lange, R. Posner, K. Pohl, C. Thierfelder, G. Grundmeier, S. Blankenburg, and W. G. Schmidt, Surf. Sci. **603**, 60 (2009).
[2]A. P. Sommer, D. Zhu, and K. Bruhne, Cryst. Growth Des. **7**, 2298 (2007).
[3]M. V. Hauf, L. H. Hess, J. Howgate, M. Dankerl, M. Stutzmann, and J. A. Garrido, Appl. Phys. Lett. **97**, 093504 (2010).
[4]K. Hirama, K. Tsuge, S. Sato, T. Tsuno, Y. Jingu, S. Yamauchi, and H. Kawarada, Appl. Phys. Express **3**, 044001 (2010).
[5]F. A. M. Koeck, R. J. Nemanich, A. Lazea, and K. Haenen, Diamond Relat. Mater. **18**, 789 (2009).
[6]D. Takeuchi, T. Makino, H. Kato, M. Ogura, N. Tokuda, K. Oyama, T. Matsumoto, I. Hirabayashi, H. Okushi, and S. Yamasaki, Appl. Phys. Express **3**, 041301 (2010).
[7]T. Yamada, S. Shikata, and C. E. Nebel, J. Appl. Phys. **107**, 013705 (2010).

[8]H. Kawarada and A. R. Ruslinda, Phys. Status Solidi A **208**, 2005 (2011).
[9]N. Yang, H. Uetsuka, and C. E. Nebel, Adv. Funct. Mater. **19**, 887 (2009).
[10]B. van Grinsven, N. Vanden Bon, H. Strauven, L. Grieten, M. Murib, K. Jimenez Monroy, S. D. Janssens, K. Haenen, M. J. Schoning, V. Vermeeren, M. Ameloot, L. Michiels, R. Thoelen, W. De Ceuninck, and P. Wagner, ACS Nano **6**, 2712 (2012).
[11]M. Dankerl, M. Tosun, M. Stutzmann, and J. A. Garrido, Appl. Phys. Lett. **100** (2012).
[12]F. Franks and D. J. G. Ives, Q. Rev. Chem. Soc. **20**, 1 (1966).
[13]S. Dixit, J. Crain, W. C. K. Poon, J. L. Finney, and A. K. Soper, Nature (London) **416**, 829 (2002).
[14]J. Guo, Y. Luo, A. Augustsson, S. Kashtanov, J. Rubensson, D. K. Shuh, H. Agren, and J. Nordgren, Phys. Rev. Lett. **91**, 157401 (2003).
[15]S. K. Allison, J. P. Fox, R. Hargreaves, and S. P. Bates, Phys. Rev. B **71**, 024201 (2005).
[16]S. M. Mejia, M. J. L. Mills, M. S. Shaik, F. Mondragon, and P. L. A. Popelier, Phys. Chem. Chem. Phys. **13**, 7821 (2011).
[17]Y. Kanda, S. Iwasaki, and K. Higashitani, J. Colloid Interface Sci. **216**, 394 (1999).
[18]P. de Gennes, F. Brochard-Wyart, and D. Quere, *Capillarity and Wetting Phenomena* (Springer-Verlag, New York, 2004).
[19]S. D. Janssens, P. Pobedinskas, J. Vacik, V. Petrakova, B. Ruttens, J. D'Haen, M. Nesladek, K. Haenen, and P. Wagner, New J. Phys. **13**, 083008 (2011).
[20]D. Y. Kim, J. Wang, J. Yang, H. W. Kim, and G. M. Swain, J. Phys. Chem. C **115**, 10026 (2011).
[21]G. Vazquez, E. Alvarez, and J. M. Navaza, J. Chem. Eng. Data **40**, 611 (1995).
[22]L. Chen and F. C. Hong, Diamond Relat. Mater. **12**, 968 (2003).
[23]J. P. Perdew and Y. Wang, Phys. Rev. B **45**, 1324 (1992).
[24]H. J. Monkhorst and J. D. Pack, Phys. Rev. B **13**, 5188 (1976).
[25]F. Ortmann, F. Bechstedt, and W. G. Schmidt, Phys. Rev. B **73**, 205101 (2006).
[26]K. Larsson and J. Ristein, J. Phys. Chem. B **109**, 10304 (2005).
[27]B. G. Pfrommer, M. Cote, S. G. Louie, and M. L. Cohen, J. Comput. Phys. **131**, 233 (1997).
[28]A. F. Azevedo, J. T. Matsushima, F. C. Vicentin, M. R. Baldan, and N. G. Ferreira, Appl. Surf. Sci. **255**, 6565 (2009).
[29]D. Petrini and K. Larsson, J. Phys. Chem. C **112**, 3018 (2008).